論文 / 著書情報
Article / Book Information

Title	Analysis of Hanle-effect signals observed in Si-channel spin accumulation devices
Authors	Y. Takamura,T. Akushichi,A. Sadono,T. Okishio,Y. Shuto,S. Sugahara
Citation	J. Appl. Phys., vol. 115, no. 17,
発行日/Pub. date	2014, 4
公式ホームページ /Journal home page	http://jap.aip.org/
権利情報/Copyright	Copyright (c) 2014 American Institute of Physics

Analysis of Hanle-effect signals observed in Si-channel spin accumulation devices

Yota Takamura, Taiju Akushichi, Adiyudha Sadano, Takao Okishio, Yusuke Shuto, and Satoshi Sugahara

Citation: Journal of Applied Physics **115**, 17C307 (2014); doi: 10.1063/1.4868502
View online: http://dx.doi.org/10.1063/1.4868502
View Table of Contents: http://scitation.aip.org/content/aip/journal/jap/115/17?ver=pdfcov
Published by the AIP Publishing

Analysis of Hanle-effect signals observed in Si-channel spin accumulation devices

Yota Takamura,[1,2,a)] Taiju Akushichi,[1] Adiyudha Sadano,[1] Takao Okishio,[1] Yusuke Shuto,[1] and Satoshi Sugahara[1,b)]
[1]*Imaging Science and Engineering Laboratory, Tokyo Institute of Technology, 4259 Nagatsuta-cho, Midori-ku, Yokohama 226-8503, Japan*
[2]*Department of Physical Electronics, Tokyo Institute of Technology, 2-12-1, Ookayama, Meguro-ku, Tokyo 152-8552, Japan*

(Presented 5 November 2013; received 27 September 2013; accepted 17 December 2013; published online 10 April 2014; publisher error corrected 14 April 2014)

We reexamined curve-fitting analysis for spin-accumulation signals observed in Si-channel spin-accumulation devices, employing widely-used Lorentz functions and a new formula developed from the spin diffusion equation. A Si-channel spin-accumulation device with a high quality ferromagnetic spin injector was fabricated, and its observed spin-accumulation signals were verified. Experimentally obtained Hanle-effect signals for spin accumulation were not able to be fitted by a single Lorentz function and were reproduced by the newly developed formula. Our developed formula can represent spin-accumulation signals and thus analyze Hanle-effect signals. [http://dx.doi.org/10.1063/1.4868502]

Spin dynamics in Si channels is one of the most important concerns for silicon spintronics.[1–15] Various analysis techniques based on the Hanle-effect and its related phenomena in spin-valve transistors,[6,7] four-terminal (4T) nonlocal devices[8,11–13] and three-terminal (3T) spin-accumulation devices[9–15] have been applied to analyze spin-injection/transport behaviors. In particular, the Hanle effect of spin-polarized electrons injected in Si channels employing 3T spin-accumulation devices has been widely used to investigate spin injection phenomena.[9–15] In this technique, spin-dependent chemical potential induced by spin injection from the ferromagnetic (FM) electrode of a 3T spin-accumulation device is measured using the identical FM electrode. When a magnetic field B is applied perpendicular to the magnetization of the FM electrode, the chemical potential is varied due to the dephasing effect caused by Larmor precession of the spin-polarized electrons accumulated in the Si channel, which causes a peak-shape detected signal, called a Hanle-effect curve (or more simply *Hanle curve*). The spin-accumulation behaviors, such as spin lifetime, are expected to easily be analyzed from the Hanle-effect curve.

In general, Hanle-effect curves are analyzed by curve-fitting using a single Lorentz function based on a one-dimensional (1D) spin diffusion model along the FM contact interface. However, controversy has arisen over the origin of the experimentally observed spin accumulation signals. This is because spin-polarized electrons trapped in the interface (or tunnel barrier) between the FM contact and the semiconductor channel can generate a Lorentz-type signal.[16,17] Furthermore, Aoki *et al*. recently reported that their observed spin-accumulation signals consisted of at least two Lorentz components having different FWHMs and that the behavior of the narrower FWHM component was consistent with that of spin signals obtained from 4T nonlocal spin-transport measurements.[13]

In this paper, we reexamined curve-fitting analysis for Hanle-effect signals observed in Si-channel spin-accumulation devices. Hanle-effect signals for spin accumulation were closely fitted by a correctly developed formula based on the spin diffusion equation.

Hanle-effect signals were originally formulated[18] for optically excited spin-polarized electrons in semiconductors, which is expressed as the effective spin density $S_{\mathrm{opt}}(B)$ by the following equation:

$$S_{\mathrm{opt}}(B) = \int_0^{\infty} s_{\mathrm{opt}}(t)\cos\omega_L t\mathrm{d}t, \tag{1}$$

where $s_{\mathrm{opt}}(t)$ represents the spin density defined by $n_{\uparrow} - n_{\downarrow}$ using spin-up electron density $n_{\uparrow}$ and spin-down electron density $n_{\downarrow}$ and ω_{L} the Larmor frequency given by $g\mu_B B/\hbar$ (in which g is the g-factor, μ_{B} the Bohr magnetron, and $\hbar$ the reduced Planck constant). Expression for Hanle-effect signals of electrically injected spin-polarized electrons in semiconductor channels can be developed as follows: Figure 1 shows the model structure for the FM electrode of 3T spin-accumulation devices in which an 1D diffusion model along the FM contact interface is employed. The diffusion equation for spin-polarized electrons injected in the channel is expressed as

$$\frac{\partial s(x,t)}{\partial t} = D\frac{\partial^2 s(x,t)}{\partial x^2} - \frac{s(x,t)}{\tau_{\mathrm{sf}}}, \tag{2}$$

where D is the diffusion constant for electrons and τ_{sf} the spin lifetime. Using the initial and boundary conditions of $s(x, 0) = 0$ $(0 \le x < \infty)$ and $s(0, t) = s_0\delta(t)$ $(t \ge 0)$, in which s_0 is the constant that is related to the spin-polarization of

a)Electronic mail: takamura@spin.pe.titech.ac.jp.
b)Electronic mail: sugahara@isl.titech.ac.jp.

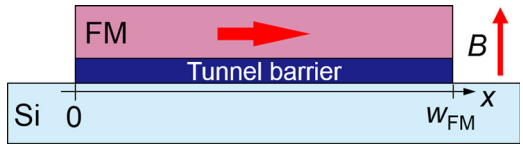

FIG. 1. Model structure for the FM electrode of 3T spin-accumulation devices.

injected electrons in the channel, the impulse response[4,5] $s_I(x,t)$ of Eq. (2) is given by

$$s_I(x,t) = s_0 \frac{x}{\sqrt{4\pi D t^3}} e^{-\frac{x^2}{4Dt}} e^{-\frac{t}{\tau_{sf}}}. \quad (3)$$

This solution is different from the widely used formula[9–15,19,20] for Hanle-effect analysis, as discussed later. When a perpendicular magnetic field B is applied to the device, the injected spin-polarized electrons precess with ω_L. In consideration of this spin precession, the spin density $S(x,B)$ at x under the steady state condition, in which the spin-polarized electrons are injected at $x=0$, can be expressed using the ordinary convolution integral

$$S(x,B) = \lim_{t\to\infty} \int_0^t s_I(x,t-t')\cos\omega_L(t-t')u(t')\mathrm{d}t', \quad (4)$$

where $u(t)$ is the unit step function. Equation (4) can easily be simplified as

$$S(x,B) = \int_0^\infty s_I(x,t)\cos\omega_L t \mathrm{d}t. \quad (5)$$

Note that this has exactly the same form as Eq. (1). Here, it is also worth noting that although the following solution $s'_I(x,t)$ is widely used[9–15,19,20] as $s_I(x,t)$ in Eqs. (4) and (5), this is not adequate

$$s'_I(x,t) = s'_0 \frac{1}{\sqrt{4\pi D t}} e^{-\frac{x^2}{4Dt}} e^{-\frac{t}{\tau_{sf}}}. \quad (6)$$

This is because $s'_I(x,t)$ is the solution of Eq. (2) for the initial condition of $s(x,0)=s'_0\delta(x)$ $(-\infty<x<\infty)$ and thus this solution is not appropriate for the convolution integral with respect to t-domain (see Eq. (4)). In this case, the convolution integral is needed to be performed in x-domain.[21] In addition, the impulse response $n'_I(x,t)$ for carrier density given by $s'_I(x,t)$ with $\tau_{sf}=\infty$ and the replacement of s'_0 by n'_0 (which is the total number of electrons injected at $x=0$.) cannot satisfy carrier conservation, i.e., $\int_0^\infty n'_I(x,t)\mathrm{d}t$ diverges for any x. The carrier conservation can be established by integration with respect to x-domain, i.e., $\int_{-\infty}^{\infty} n'_I(x,t)\mathrm{d}x = n'_0$. Note that although $\int_0^\infty s'_I(x,t)\mathrm{d}t$ can converge, this is due to the decay factor $e^{-\frac{t}{\tau_{sf}}}$. On the other hand, the carrier density $n_I(x,t)$ given by $s_I(x,t)$ with $\tau_{sf}=\infty$ and the replacement of s_0 by n_0 (which represents the total number of electrons injected at $t=0$.) satisfies carrier conservation, i.e., $\int_0^\infty n_I(x,t)\mathrm{d}t = n_0$ for any x. The corresponding spin conservation is also established for $s_I(x,t)$ with $\tau_{sf}=\infty$. The behaviors of $n_I(x,t)$ and $s_I(x,t)$ clearly show the validity of Eq. (3) adaptable to Eq. (5).

Spin accumulation density $S_{SA}(B)$ per unit width can be obtained by the following convolution integral of the spin density $S(x,B)$:

$$S_{SA}(B) = \frac{1}{w_{FM}} \int_0^{w_{FM}} \int_0^x S(x-x',B)u(x')\mathrm{d}x'\mathrm{d}x, \quad (7)$$

in which the convolution integrates over the FM electrode width (w_{FM}). Since $S_{SA}(B)$ is proportional to the chemical potential difference underneath the FM contact, $S_{SA}(B)$ can represent Hanle-effect signals for the spin accumulation in the channel. The curve shape of $S_{SA}(B)$ expressed by Eq. (7) is different from the Lorentz function, as described later.

Fundamental characteristics of Hanle-effect signals observed in 3T spin-accumulation devices can be analyzed using Eq. (7). The Hanle-effect curves of the devices depend on the size (w_{FM}) of the FM electrode. Figure 2(a) shows calculated peak intensity ($S_{SA}(0)$) of Hanle-effect curves as a function of w_{FM} for a range of τ_{sf} from 10 ps to 10 ns, in which D is set to 10 cm^2/s. These τ_{sf} values correspond to spin diffusion length λ_{sf} $(=\sqrt{D\tau_{sf}})$ of 0.32–3.2 μm. The peak intensities increase with increasing w_{FM} and then are saturated. This w_{FM}-dependence can be attributed to the spin relaxation during the diffusion as follows: When w_{FM} is shorter than λ_{sf} or comparable with λ_{sf}, injected spin-polarized electrons can diffuse over w_{FM} with their spin-polarization keeping. Consequently, $S_{SA}(0)$ increase with increasing w_{FM}. On the other hand, when w_{FM} is larger than λ_{sf}, injected electrons cannot retain their spin-polarization for the diffusion length longer than λ_{sf}, i.e., the spatial range of the spin accumulation from the single spin injection point is limited at around λ_{sf}. This results in the constant spin accumulation signal that is independent of w_{FM}. Figure 2(b) shows the normalized $S_{SA}(B)$ curves as a function of B for $w_{FM}=0.1$–100 μm, in which τ_{sf} and D are set to 100 ps and 10 cm^2/s, respectively (note that this parameter set corresponds to $\lambda_{sf}=0.32$ μm). Sufficiently, longer w_{FM} than λ_{sf} is required to obtain w_{FM}-independent Hanle-effect curves (which are indispensable to extract spin lifetime from the curve analysis). This is because sufficiently long diffusion length is required for the dephasing. Therefore, to accurately determine spin lifetime from fitting analysis of Hanle-effect curves, the condition of $w_{FM} \gg \lambda_{sf}$ is required.

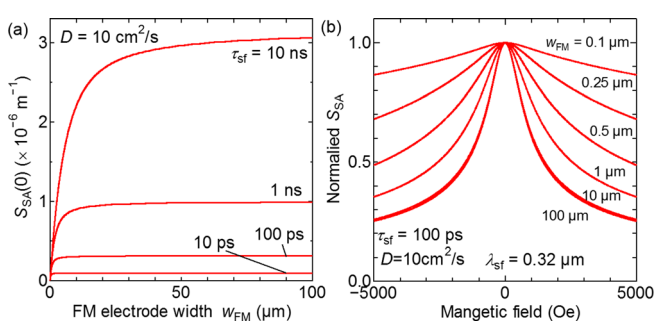

FIG. 2. (a) Calculated peak intensity ($S_{SA}(0)$) of Hanle-effect signals as a function of w_{FM} for $D=10\,cm^2/s$ and $\tau_{sf}=10$ ps–10 ns. (b) Normalized $S_{SA}(B)$ curves as a function of B for $w_{FM}=0.1$–100 μm.

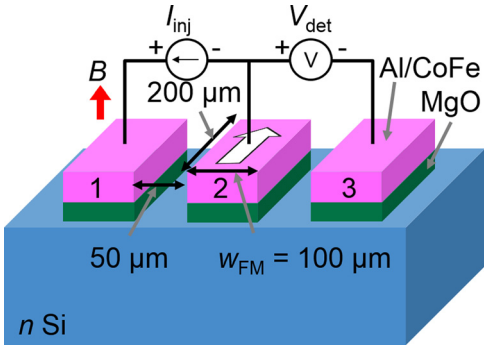

FIG. 3. Schematic of a fabricated 3T spin-accumulation device.

As noted previously, these S_{SA} curves cannot be fitted by a single Lorentz function. Experimentally observed Hanle-effect curves using a Si-channel spin-accumulation device with a high quality ferromagnetic spin injector were closely fitted by Eq. (7), as shown below. Figure 3 shows a schematic of a fabricated 3T spin-accumulation device. The fabrication procedure is as follows. An FM tunnel contact for the spin-injector of the device was formed using an ultra-high vacuum multi-chamber system equipped with radical oxidation, metal sputtering, and molecular beam deposition (MBD) systems. First, an n^+-Si substrate (phosphorous--doped; 4×10^{19} cm^{-3}) was chemically cleaned and then thermally cleaned in an ultrahigh vacuum. An Mg film was deposited on the substrate by sputtering, and then the sample was transferred into the radical oxidation chamber without breaking an ultrahigh vacuum. Radical oxidation of the Mg film was performed at room temperature for 30 min with an RF power of 200 W. Successively, annealing was carried out at 400 °C for 30 min under radical oxygen exposure. After the sample was transferred to the MBD chamber, a CoFe layer was deposited on the sample at room temperature, and then the surface was covered by an Al capping layer. The thicknesses of the CoFe and Al layers were 30 nm and 10 nm, respectively. This stacked structure was patterned into rectangular-shape contacts (100 μm $\times$ 200 μm) by Ar ion milling, and then the sample surface was passivated by an SiO_2 film. The distance between the adjacent electrodes is 50 μm. Finally, contact holes were fabricated and Al pads were formed.

Measurement setup for Hanle-effect curves of the fabricated 3T spin-accumulation device is also shown in Fig. 3. Spin-polarized electrons were injected from the contact 2 by applying a voltage bias between the contacts 1 and 2. The chemical potentials underneath the contact 2 were measured by a voltmeter between the contacts 2 and 3. A magnetic field B was applied perpendicular to the sample surface.

Gray open circles in Fig. 4 show spin-accumulation signals measured by the fabricated device at 10 K with an injection current of 10 mA. The signal was not able to be fitted by a single Lorentz function, as shown by green dotted and blue dashed curves in the figure, although the Lorentz function with a narrow (broad) FWHM could fit the signal around the peak center (edge). The signal was reproduced by two Lorentz functions having different FWHMs. Since these components exhibited the same bias- and temperature-

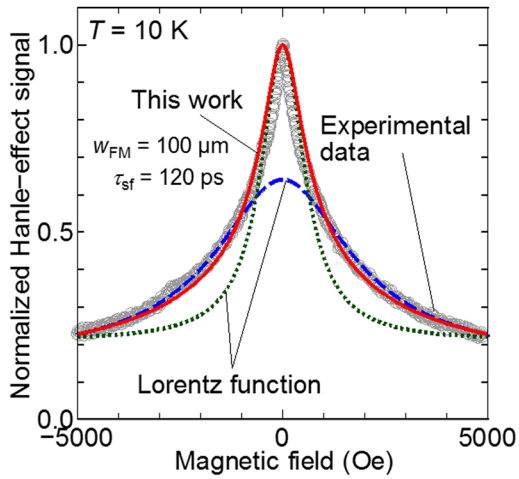

FIG. 4. Hanle-effect signals measured at temperature of 10 K with injection current of 10 mA. Lorentz and our developed fitting functions are also shown.

dependence, they were considered to be caused by the same origin, i.e., the deconvolution would not be adequate. On the other hand, a single curve of our developed formula (Eq. (7)) reproduced the measured signal, as shown by a red solid curve in the figure. Using our developed formula, τ_{sf} was estimated to 120 ps from the fitting result when D was assumed to be 10 cm^2/s. Resulting λ_{sf} was 0.35 μm that was much shorter than w_{FM} (100 μm). Note that recently a few groups have also been observed Hanle-effect signals similar to our observed signal. Their signal also cannot be fitted by a single Lorentz function[13,22] and is likely to be fitted by our developed formula. These reports could support the validity of the formula of Eq. (3). Our developed formula can represent spin-accumulation signals and thus use to verify Hanle-effect curves observed in spin-accumulation devices.

This study was partly supported by Kanagawa Academy of Science and Technology (KAST).

[1]S. Sugahara, IEE Proc.-Circuits, Devices-Syst. **152**, 355 (2005).
[2]S. Sugahara, Phys. Status Solidi C **3**, 4405 (2006).
[3]S. Sugahara and J. Nitta, Proc. IEEE **98**, 2124 (2010).
[4]Y. Takamura and S. Sugahara, J. Appl. Phys. **111**, 07C323 (2012).
[5]Y. Takamura and S. Sugahara, IEEE Magn. Lett. **2**, 3000404 (2011).
[6]I. Appelbaum *et al.*, Nature **447**, 295 (2007).
[7]B. Huang *et al.*, Phys. Rev. Lett. **99**, 177209 (2007).
[8]O. M. J. van 't Erve *et al.*, Appl. Phys. Lett. **91**, 212109 (2007).
[9]S. P. Dash *et al.*, Nature **462**, 491 (2009).
[10]C. H. Li *et al.*, Nat. Commun. **2**, 245 (2011).
[11]T. Sasaki *et al.*, Appl. Phys. Lett. **98**, 012508 (2011).
[12]T. Suzuki *et al.*, Appl. Phys. Express **4**, 023003 (2011).
[13]Y. Aoki *et al.*, Phys. Rev. B **86**, 081201(R) (2012).
[14]R. Jansen *et al.*, Phys. Rev. B **82**, 241305 (2010).
[15]R. Jansen *et al.*, Semicond. Sci. Technol. **27**, 083001 (2012).
[16]M. Tran *et al.*, Phys. Rev. Lett. **102**, 036601 (2009).
[17]O. Txoperena *et al.*, Appl. Phys. Lett. **102**, 192406 (2013).
[18]M. I. Dyakonov and V. I. Perel, in *Optical Orientation*, edited by F. Meier and B. P. Zakharchenya (North Holland, Amsterdam, 1984), pp. 39–47.
[19]F. J. Jedema *et al.*, Nature **416**, 713 (2002).
[20]X. Lou *et al.*, Phys. Rev. Lett. **96**, 176603 (2006).
[21]S. J. Farlow, *Partial Differential Equations for Scientists and Engineers* (Dover Publications, New York, 1993).
[22]M. Ishikawa *et al.*, in *Extended Abstracts of the 2013 International Conference on Solid State Devices and Materials*, Fukuoka, Japan, 24–27 September (The Japan Society of Applied Physics, 2013), pp. 380–381, PS-12-2.